

Towards Multimodal Human Intention Understanding Debiasing via Subject-Deconfounding

Dingkang Yang^{1,3†}, Dongling Xiao², Ke Li², Yuzheng Wang¹, Zhaoyu Chen¹,
Jinjie Wei¹, and Lihua Zhang^{1,3,4✉}

¹ Academy for Engineering & Technology, Fudan University

² Tencent Youtu Lab

³ Cognition and Intelligent Technology Laboratory (CIT Lab)

⁴ Engineering Research Center of AI and Robotics, Ministry of Education, China

Abstract. Multimodal intention understanding (MIU) is an indispensable component of human expression analysis (*e.g.*, sentiment or humor) from heterogeneous modalities, including visual postures, linguistic contents, and acoustic behaviors. Existing works invariably focus on designing sophisticated structures or fusion strategies to achieve impressive improvements. Unfortunately, they all suffer from the subject variation problem due to data distribution discrepancies among subjects. Concretely, MIU models are easily misled by distinct subjects with different expression customs and characteristics in the training data to learn subject-specific spurious correlations, significantly limiting performance and generalizability across uninitiated subjects. Motivated by this observation, we introduce a recapitulative causal graph to formulate the MIU procedure and analyze the confounding effect of subjects. Then, we propose SuCI, a simple yet effective causal intervention module to disentangle the impact of subjects acting as unobserved confounders and achieve model training via true causal effects. As a plug-and-play component, SuCI can be widely applied to most methods that seek unbiased predictions. Comprehensive experiments on several MIU benchmarks clearly demonstrate the effectiveness of the proposed module.

Keywords: Human intention understanding · Multimodal learning

1 Introduction

“You must never let the appearance of any subject affect your judgment.”

—Sherlock Holmes, The Sign of the Four

As a research hotspot that combines linguistic [3] and non-verbal behaviors (*e.g.*, visual [6] and acoustic [37] modalities), multimodal intention understanding (MIU) has attracted significant attention from computer vision [4, 10, 48],

[†]Work done during the internship at Tencent Youtu Lab. [✉]Corresponding author.

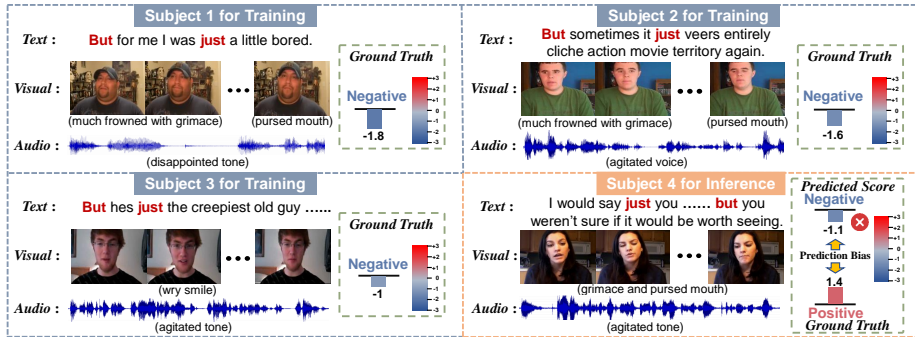


Fig. 1: Examples on the MOSI benchmark [61] illustrate the subject variation problem. Multimodal expressions from four subjects potentially convey distinct semantic correlations due to their different customs and styles in expressing sentiments. Training with samples collected from the subjects (1, 2, 3) invariably results in the SOTA model [21] learning spurious connections between subject-specific semantics and negative sentiment polarity. In this case, the differences between the subject-specific relations captured via the multimodal manner and the characteristics of subject 4 would lead to the subject-related prediction bias.

natural language processing [35, 41], and speech recognition communities [49, 52] in recent years. Thanks to the progressive development of multimodal language benchmarks [13, 60, 61], extensive studies [9, 12, 18, 23, 27, 28, 34, 36, 38, 42, 43, 58, 59] have presented impressive multimodal models on training data containing distinct subjects, diverse topics, and different modalities. Despite the achievements of previous approaches by exploiting representation learning architectures [9, 23, 48] and fusion strategies [28, 42, 59], they invariably suffer from a prediction bias when applied to testing samples of new subjects.

The harmful prediction bias is mainly caused by the subject variation problem. Specifically, different subjects’ expression styles and behaviors (*e.g.*, facial expressions or acoustic information) from the training data are highly idiosyncratic in social communication, affected by the subjects’ customs or culture [20]. Once well-designed models are trained on such data, subject-specific semantic correlations (*e.g.*, particular facial action unit co-occurrence [5]) would inexorably affect performance and generalizability. Worse still, the spurious connections between the trained models and specific subjects will be transmitted via multiple modalities when the data paradigm is extended from isolated to multimodal situations. Recall the prominent MIU benchmarks (*e.g.*, MOSI [61] for sentiment analysis or UR_FUNNY [13] for humor detection), whose collectors advocated video-level data splitting so that segments from the same video will not appear across train, valid, and test splits. Although the trained models may avoid memorizing the average affective state of a subject [22], they cannot generalize well across uninitiated subjects. The examples in Fig. 1 provide strong evidence of this. Concretely, subjects 1, 2, and 3 tend to use sentimentally unimportant words “*but*” and “*just*” to express negative emotions. In this case, the state-of-the-art (SOTA) model [21] is misled to focus on spurious clues

from the textual utterances of the subjects and make an entirely incorrect prediction when applied to subject 4. Similar observations are found in the visual and audio modalities. For instance, the trained model erroneously takes subject-specific facial appearances (*e.g.*, “grimace and pursed mouth” from subjects 1 and 2) and acoustic behaviors (*e.g.*, “agitated tone” from subjects 2 and 3) as semantic shortcuts to infer frustrating negative sentiment polarity.

Motivated by the above observations, this paper aims to improve MIU methods by causal demystification rather than beating them. We propose a Subject Causal Intervention module (SuCI) to disentangle the impact of semantic differences among subjects from multimodal expressions. Specifically, we first formulate a universal causal graph to analyze the MIU procedure and interpret the causalities among the variables. From the causal inference perspective, the **subjects** are essentially regarded as **confounders** [11], which mislead the models to learn subject-specific semantic correlations in the training data, as well as causing prediction bias for new subjects in the inference phase. For clarity, we represent the multimodal inputs as \mathbf{X} (cause) and its corresponding predictions as \mathbf{Y} (effect). Existing MIU models aim to approximate $P(\mathbf{Y}|\mathbf{X})$ as much as possible while failing to perform unbiased predictions. Unlike conventional likelihood estimation $P(\mathbf{Y}|\mathbf{X})$, our SuCI achieves subject de-confounded training and removes subject-caused confounding effects by embracing causal intervention $P(\mathbf{Y}|do(\mathbf{X}))$ regarding the backdoor adjustment [30]. As a model-agnostic component, SuCI can be readily integrated into most MIU models to perform unbiased predictions by pursuing true causal effects among variables. We comprehensively evaluate the effectiveness of SuCI on several MIU benchmarks. Numerous experiments show that SuCI can significantly and consistently improve existing baselines, achieving new SOTA performance.

To sum up, this paper has the following contributions. **(i)** We are the first to investigate the subject variation problem in MIU tasks via a tailored causal graph and identify the subjects as confounders which misleads the models to capture subject-specific spurious correlations and cause prediction bias. **(ii)** Based on the causal theory of backdoor adjustment, we present SuCI, a subject causal intervention module to remove prediction bias and confounding effects of subjects. **(iii)** The causality-based SuCI is general and suitable for various models with distinct structures and fusion strategies.

2 Related Work

2.1 Multimodal Intention Understanding

Benefiting from available human communication resources and data, MIU benchmarks [4, 13, 60, 61] with different scales and typologies have been increasingly developed and applied in recent years. Recent MIU tasks focus on subject-centered intention understanding and behavior analysis from text, visual, and audio modalities, including but not limited to emotion recognition [28], sentiment analysis [12], and humor detection [13]. Considering the heterogeneous and asynchronous nature of multimodal languages, numerous works have presented

seminal network structures [23, 34, 38, 58], fusion strategies [36, 42, 43, 59], and representation learning paradigms [9, 19, 48, 50, 52]. For instance, Zadeh *et al.* [59] proposed a tensor fusion to capture uni-modal, bi-modal, and tri-modal interactions explicitly. Tsai *et al.* [42] designed a multimodal transformer structure to learn an adaptive process from one modality to another to capture cross-modal element dependencies. Afterward, Yang *et al.* [52] presented a factorized representation strategy to learn similarities and differences among multimodal languages. Despite substantial achievements, existing methods invariably suffer from performance bottlenecks due to subject-related prediction bias caused by the subject variation problem. In this paper, we identify subjects in MIU benchmarks as harmful confounders from a causal perspective and improve different models with the proposed SuCI.

2.2 Causal Demystification

Causal demystification as a revolutionary statistical theory aims to pursue causal effects among observed variables rather than their shallow correlations. Benefiting from the advances in learning-based technologies [25, 26, 51, 53–55], several studies exploring causality are mainly divided into two channels: causal intervention [24, 57] and counterfactual reasoning [35, 40]. Intervention [30] focuses on altering the natural tendency of the independent variable to vary with other variables to eliminate the impact of adverse effects. Counterfactuals depict imagined outcomes produced by factual variables under different treatment conditions [31]. Given the unbiased estimations provided by causal inference, it is increasingly applied to various downstream tasks such as computer vision [47, 56], natural language processing [15, 62], and reinforcement learning [7]. Recently, Sun *et al.* [39] revealed the harmful associations of text semantics in multimodal sentiment analysis through counterfactual manipulation. In contrast, we address the confounding effect from multiple modalities by embracing causal intervention, which is more generalizable and adaptable for multimodal approaches.

3 Methodology

3.1 Structural Causal Graph in MIU Tasks

To systematically diagnose the confounding effect present in MIU tasks, we first design a recapitulative causal graph to summarize the causal relationships among variables. The mainstream graphical notation following the structured causal model [32] is adopted due to its intuitiveness and interpretability. Concretely, a causal graph $\mathcal{G} = \{\mathcal{N}, \mathcal{E}\}$ is considered a directed acyclic graph, which represents how a set of variables \mathcal{N} convey causal effects through the causal links \mathcal{E} . As shown in Fig. 2(a), there are four variables in the MIU causal graph, including multimodal inputs \mathbf{X} , multimodal representations \mathbf{M} , unintended confounders \mathbf{Z} , and predictions \mathbf{Y} . Note that our causal graph applies to various MIU approaches since it is highly general, imposing no constraints on the detailed implementations. The detailed causalities are described as follows.

► **Link $Z \rightarrow X$.** Multimodal expressions from distinct subjects are recorded to produce multimodal inputs \mathbf{X} , where \mathbf{X} is a generalized definition of text \mathbf{X}_t , visual \mathbf{X}_v , and audio \mathbf{X}_a modalities for simplicity, *i.e.*, $\mathbf{X} = \{\mathbf{X}_t, \mathbf{X}_v, \mathbf{X}_a\}$. Subjects are identified as harmful confounders Z due to the subject-related prediction bias caused by different human expression customs and differences [13, 60]. In this case, Z with heterogeneous attributes is a collective denomi-

nation of multimodal confounding sources. For training inputs \mathbf{X} , Z determines the subject-related biased content that is recorded, *i.e.*, $Z \rightarrow X$.

► **Link $Z \rightarrow M \leftarrow X$.** M denotes the refined multimodal representations extracted by any MIU model, which acts as a mediator before the final classifier. The causal path $Z \rightarrow M$ indicates detrimental Z confounding models to capture subject-specific characteristics embedded in M to produce spurious semantic correlations. Several intuitive examples are the semantically unimportant words from the text modality and the agitated tones from the audio modality in Fig. 1. Furthermore, M contains universal multimodal feature semantics from \mathbf{X} that can be reflected via the causal link $X \rightarrow M$.

► **Link $M \rightarrow Y \leftarrow Z$.** The causal path $M \rightarrow Y$ reveals that the impure M confounded by Z further impacts the final predictions Y of downstream MIU tasks. Meanwhile, adverse confounders’ prior information in the training data implicitly interferes with Y along the link $Z \rightarrow Y$.

According to the causal theory [30], the confounders Z are the common cause of X and corresponding predictions Y . The positive effect of the subject-agnostic multimodal semantics provided by M follows the desired causal path $X \rightarrow M \rightarrow Y$, which we aim to achieve and pursue. Unfortunately, Z causes subject-related prediction bias and misleads trained models to learn subject-specific misleading semantics rather than pure causal effects, leading to biased predictions on uninitiated subjects. The detrimental effects follow the backdoor paths $X \leftarrow Z \rightarrow Y$ and $X \leftarrow Z \rightarrow M \rightarrow Y$.

3.2 Causal Intervention via Backdoor Adjustment

Following the causal graph in Fig. 2(a), the MIU model relies on the likelihood $P(Y|\mathbf{X})$ for predictions that suffer from backdoor effects. $P(Y|\mathbf{X})$ can be decomposed by the Bayes rule as follows:

$$P(\mathbf{Y}|\mathbf{X}) = \sum_z P(\mathbf{Y}|\mathbf{X}, M = \mathcal{F}_m(\mathbf{X}, z))P(z|\mathbf{X}), \tag{1}$$

where $\mathcal{F}_m(\cdot)$ denotes any vanilla MIU model to learn the multimodal representations M . z is a stratum of confounders (*i.e.*, a subject), which introduces

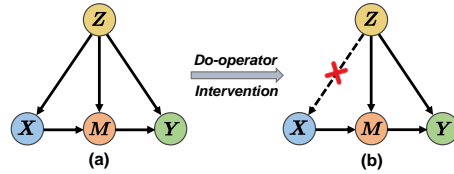


Fig. 2: The proposed causal graph explains the causal effects of the MIU procedure. Nodes denote variables and arrows denote the direct causal effects. (a) The conventional likelihood estimation $P(\mathbf{Y}|\mathbf{X})$. (b) The causal intervention $P(\mathbf{Y}|do(\mathbf{X}))$.

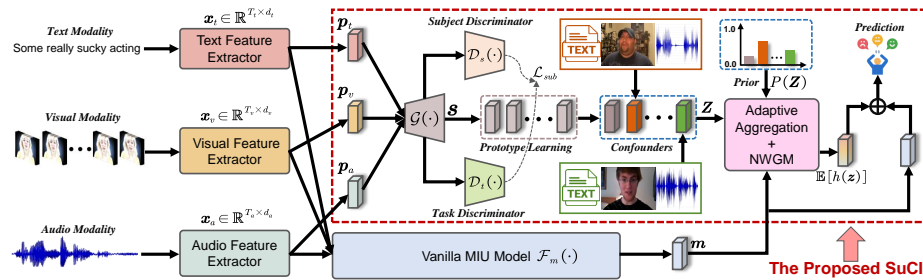


Fig. 3: A general MIU pipeline for the subject de-confounded training. The red dotted box shows the core component that achieves the approximation to causal intervention: our SuCI. SuCI can be readily integrated into the vanilla MIU model via backdoor adjustment to mitigate subject-specific spurious correlations and achieve debiased predictions in downstream MIU tasks.

the observational bias via $P(\mathbf{z}|\mathbf{X})$. Theoretically, an ideal solution would be to collect massive data samples to ensure that subjects with different expression characteristics are included in the training and testing sets. However, this way is unrealistic due to human-bounded rationality and social ethics issues [17]. To address this, we embrace causal intervention $P(\mathbf{Y}|do(\mathbf{X}))$ to interrupt the adverse effects propagating between \mathbf{X} and \mathbf{Y} along the backdoor paths via the backdoor adjustment theory [30]. The $do(\cdot)$ operator is an efficient approximation to implement the empirical intervention [11]. In our case, backdoor adjustment means measuring the causal effect of each stratum in the subject confounders and then performing a weighted integration based on the prior proportions of samples from different subjects in the training data to estimate the average causal effect. From Fig. 2(b), the impact from \mathbf{Z} to \mathbf{X} is cut off since the model would enable the subject prototype as the confounder in each stratum to contribute equally to the predictions \mathbf{Y} by $P(\mathbf{Y}|do(\mathbf{X}))$. Eq. (1) with the intervention is formulated as follows:

$$P(\mathbf{Y}|do(\mathbf{X})) = \sum_{\mathbf{z}} P(\mathbf{Y}|\mathbf{X}, \mathbf{M} = \mathcal{F}_m(\mathbf{X}, \mathbf{z}))P(\mathbf{z}). \quad (2)$$

Intuitively, the model is no longer disrupted by subject-specific spurious correlations in backdoor paths since \mathbf{z} no longer affects \mathbf{X} . $P(\mathbf{z})$ is the prior probability that depicts the proportion of each \mathbf{z} in the whole.

3.3 Subject De-confounded Training with SuCI

We present a plug-in Subject Causal Intervention module (SuCI) to convert the theoretical intervention in Eq. (2) into a practical implementation. As Fig. 3 shows, SuCI can be readily integrated into the vanilla MIU model to estimate $P(\mathbf{Y}|do(\mathbf{X}))$ through the subject de-confounded training. The implementation details are as follows.

Subject-specific Feature Disentanglement. How to effectively disentangle subject-specific features from heterogeneous modalities is key to determining confounders. Considering that subject-related spurious semantics are usually distributed among different frames of multimodal sequences [48], we first devise a dynamic fusion mechanism to aggregate the frame-level semantic clues. Let the text, visual, and audio modality sequences from the corresponding feature extractors be denoted as $\mathbf{x}_t \in \mathbb{R}^{T_t \times d_t}$, $\mathbf{x}_v \in \mathbb{R}^{T_v \times d_v}$, and $\mathbf{x}_a \in \mathbb{R}^{T_a \times d_a}$, respectively, where $T_{(\cdot)}$ is the frame length and $d_{(\cdot)}$ is the embedding dimension. The dynamic fusion procedure is formulated as follows:

$$\xi_m = \phi(\mathbf{x}_m \mathbf{w}_{x_m} + \mathbf{b}_{x_m}) \in \mathbb{R}^{T_m \times 1}, \quad (3)$$

$$\mathbf{p}_m = \xi_m^T \mathbf{x}_m \in \mathbb{R}^{d_m}, \quad (4)$$

where $m \in \{t, v, a\}$, $\phi(\cdot)$ is the softmax function, $\mathbf{w}_{x_m} \in \mathbb{R}^{d_m \times 1}$, and $\mathbf{b}_{x_m} \in \mathbb{R}^{T_m \times 1}$ are the learnable parameters. The attention vectors ξ_m adaptively capture salient semantics and produce informative representations \mathbf{p}_m based on the contributions of different frames. Subsequently, we introduce an adversarial strategy to disentangle the subject-specific semantics and avoid the task-related semantics. The design philosophy is to distill pure subject features for better confounder construction. Specifically, a subject generator $\mathcal{G}(\cdot; \theta_{\mathcal{G}})$ is presented to project \mathbf{p}_t , \mathbf{p}_v , and \mathbf{p}_a of multimodal utterances from the subject into a common space to yield a subject-specific feature \mathbf{s} , expressed as follows:

$$\mathbf{s} = \mathcal{G}([\mathbf{p}_t, \mathbf{p}_v, \mathbf{p}_a]; \theta_{\mathcal{G}}) \in \mathbb{R}^{d_s \times 1}, \quad (5)$$

where $[\cdot, \cdot]$ stands for the concatenation operator and $d_s = d_t + d_v + d_a$. The generator is implemented as a two-layer perceptron with the GeLU [14] activation. \mathbf{s} is distilled by the following optimization objective:

$$\mathcal{L}_{sub} = \mathcal{CE}(\mathcal{D}_s(\mathbf{s}; \theta_{\mathcal{D}_s}), y_s) + \mathcal{MSE}(\mathcal{D}_t(\mathbf{s}; \theta_{\mathcal{D}_t}), \frac{1}{C_t}), \quad (6)$$

where $\mathcal{CE}(\cdot)$ and $\mathcal{MSE}(\cdot)$ represent the cross-entropy loss and mean squared error loss, respectively. $\mathcal{D}_s(\cdot; \theta_{\mathcal{D}_s})$ and $\mathcal{D}_t(\cdot; \theta_{\mathcal{D}_t})$ are the subject discriminator and task discriminator parameterized by $\theta_{\mathcal{D}_s}$ and $\theta_{\mathcal{D}_t}$, respectively, which consist of feed-forward neural layers. y_s is the subject label determined by the dataset’s subject index. C_t is the number of categories in downstream MIU tasks. In Eq. (6), \mathbf{s} is supervised to encourage the output logits of the task discriminator to be equally distributed among all prediction categories to exclude task-related semantic information. Also, the subject discriminator is optimized to ensure that \mathbf{s} belongs to a given subject, *i.e.*, contains subject-specific semantics.

Confounder Construction. Confounder construction aims to make the model measure the causal effect of subject confounders among different strata during training to avoid subject-related prediction bias. Considering that subject features are similar within the same stratum and different across strata [30], we utilize all the features from a specific subject as the subject prototype, which represents the universal attributes of confounders in a specific stratum. Concretely,

we maintain a memory cache for each subject during training to store and update the subject prototype as a confounder, which is computed as $\mathbf{z}_i = \frac{1}{N_i} \sum_{k=1}^{N_i} \mathbf{s}_k^i$. N_i is the number of training samples for the i -th subject, and \mathbf{s}_k^i denotes the k -th feature of the i -th subject. \mathbf{z}_i is updated at the end of each epoch. In practice, each \mathbf{z}_i is initialized by the uniform distribution to ensure stable training at the first epoch. Based on the number of subjects N_c , a stratified confounder dictionary is constructed, which is formulated as $\mathbf{Z} = [\mathbf{z}_1, \mathbf{z}_2, \dots, \mathbf{z}_{N_c}]$.

Intervention Instantiation. Estimating $P(\mathbf{Y}|do(\mathbf{X}))$ in practice is high overhead since it requires the forward computation of \mathbf{X} and \mathbf{z} for each pair. To reduce the overhead, we introduce the Normalized Weighted Geometric Mean (NWGM) [46] to achieve feature-level approximation for intervention instantiation:

$$P(\mathbf{Y}|do(\mathbf{X})) \stackrel{\text{NWGM}}{\approx} P(\mathbf{Y}|\mathbf{X}, \mathbf{M} = \sum_{\mathbf{z}} \mathcal{F}_m(\mathbf{X}, \mathbf{z})p(\mathbf{z})). \quad (7)$$

In this case, causal intervention makes \mathbf{X} contribute fairly to the predictions of \mathbf{Y} by incorporating every \mathbf{z} . We parameterize a network model to approximate Eq. (7) as:

$$P(\mathbf{Y}|do(\mathbf{X})) = \mathbf{W}_m \mathbf{m} + \mathbf{W}_h \mathbb{E}[h(\mathbf{z})], \quad (8)$$

where $\mathbf{W}_m \in \mathbb{R}^{d_h \times d}$ and $\mathbf{W}_h \in \mathbb{R}^{d_h \times d_s}$ are the learnable parameters. $\mathbf{m} \in \mathbb{R}^{d \times 1}$ is the multimodal representation produced by the vanilla MIU model. The above approximation is reasonable since the effect on \mathbf{Y} is attributed to \mathbf{M} and \mathbf{Z} in the MIU causal graph. Then, $\mathbb{E}[h(\mathbf{z})]$ is approximated as an adaptive aggregation for all confounders according to the backdoor adjustment of Sec. 3.2, which is formulated as follows:

$$\mathbb{E}[h(\mathbf{z})] = \sum_{i=1}^{N_c} \psi_i \mathbf{z}_i p(\mathbf{z}_i), \quad (9)$$

$$\psi_i = \phi\left(\frac{(\mathbf{W}_q \mathbf{m})^T (\mathbf{W}_k \mathbf{z}_i)}{\sqrt{d_s}}\right), \quad (10)$$

where $\mathbf{W}_q \in \mathbb{R}^{d_n \times d}$ and $\mathbf{W}_k \in \mathbb{R}^{d_n \times d_s}$ are mapping matrices. $p(\mathbf{z}_i) = \frac{N_i}{N}$, where N is the number of training samples. In practice, \mathbf{m} from one sample queries each \mathbf{z}_i in the confounder dictionary $\mathbf{Z} \in \mathbb{R}^{N_c \times d_s}$ to obtain the sample-specific attention set $\{\psi_i\}_{i=1}^{N_c}$. The intuition insight is that samples from one subject are impacted by varying degrees of confounder \mathbf{z}_i of other subjects.

Objective Optimization. The standard cross-entropy loss is employed as the task-related training objective, which is expressed as $\mathcal{L}_{task} = -\frac{1}{N_i} \sum_{t=1}^{N_i} y_t \cdot \log \hat{y}_t$, where y_t is the task-related ground truth. The overall objective function is computed as $\mathcal{L}_{all} = \mathcal{L}_{sub} + \mathcal{L}_{task}$.

4 Experiments

4.1 Benchmarks and Evaluation Metrics

Extensive experiments are conducted on three mainstream MLU benchmarks. Concretely, MOSI [61] is a multimodal human sentiment analysis dataset con-

sisting of 2,199 video segments. The standard data partitioning is 1,284 samples for training, 284 samples for validation, and 686 samples for testing. These samples contain a total of 89 distinct subjects from video blogs. Each sample is manually annotated with a sentiment score ranging from -3 to 3, including *highly negative*, *negative*, *weakly negative*, *neutral*, *weakly positive*, *positive*, and *highly positive*. **MOSEI** [60] is a large-scale human sentiment and emotion recognition benchmark containing 22,856 video clips from 1,000 different subjects and 250 diverse topics. Among these samples, 16,326, 1,871, and 4,659 samples are used as training, validation and testing sets. The sample annotation protocols used for sentiment analysis are consistent with MOSI. **UR_FUNNY** [13] is a multimodal human humor detection dataset that contains 16,514 video clips from 1,741 subjects collected by the TED portal. There are 10,598, 2,626, and 3,290 samples in the training, validation, and testing sets. Each sample provides the target punchlines and associated contexts from multimodal utterances to support the detection of subject humor/non-humor in the binary labels.

Evaluation Metrics. Following widely adopted implementations [21, 42, 48], we use the 7-class accuracy (Acc_7), binary accuracy (Acc_2), and $F1$ score to evaluate the results on MOSI and MOSEI. The standard binary accuracy (Acc_2) is utilized for evaluation on UR_FUNNY.

4.2 Model Zoo

Considering applicability and scalability, we choose five reproducible models with entirely different network structures to verify the proposed plug-in SuCI. A brief overview is as follows. Specifically, **MuT** [42] constructs multimodal transformers to learn element dependencies between pairwise modalities. **MISA** [9] captures modality-invariant and modality-specific diverse representations based on feature disentanglement. **Self-MM** [58] utilizes a self-supervised paradigm to learn additional emotion semantics from unimodal label generation. **MMIM** [12] proposes a hierarchical mutual information maximization to alleviate the loss of valuable task-related clues. **DMD** [21] designs cross-modal knowledge distillations to bridge the semantic gap among heterogeneous modalities.

4.3 Implementation Details

All models follow consistent feature extraction procedures for fair comparisons. The text feature extractor is instantiated by pre-trained Glove word embedding tool [33] to obtain 300-dimensional linguistic vectors. For MOSI & MOSEI, we use the library Facet [16] to extract an ensemble of visual features, including 35 facial action units to reflect facial gesture changes. Meanwhile, Openface [2] is utilized on UR_FUNNY to extract 75-dimensional features related to facial behaviors and expressions. The audio feature extraction is executed utilizing the software COVAREP [8] to obtain diverse acoustic attributes, where the dimensions on MOSI & MOSEI and UR_FUNNY are 74 and 81, respectively. The word-aligned data points are employed across all benchmarks. In the SuCI implementation, the hidden dimensions d_h and d_n are set to 64 and 128, respectively.

Table 1: Comparison results of different methods and SuCI-based models on the MOSI benchmark. Improved results and corresponding gains compared to vanilla methods are marked in **bold** and **red**, respectively.

Methods	$Acc_7 \uparrow$ (%)	$Acc_2 \uparrow$ (%)	$F1 \uparrow$ (%)
EF-LSTM	33.7	75.3	75.2
LF-LSTM	35.3	76.8	76.7
Graph-MFN [60]	29.6	75.4	76.6
TFN [59]	32.1	73.9	73.4
LMF [27]	32.8	76.4	75.7
MFM [43]	36.2	78.1	78.1
RAVEN [44]	33.2	78.0	76.6
MCTN [34]	35.6	79.3	79.1
TCSP [45]	-	80.9	81.0
PMR [28]	40.6	83.6	83.4
FDMER [48]	42.1	84.2	83.9
MuT [42]	39.5	82.6	82.5
MuT + SuCI	40.7 ^{+1.2}	83.4 ^{+0.8}	83.4 ^{+0.9}
MISA [9]	40.2	81.8	81.9
MISA + SuCI	41.6 ^{+1.4}	83.3 ^{+1.5}	83.1 ^{+1.2}
Self-MM [58]	41.6	83.9	84.1
Self-MM + SuCI	42.0 ^{+0.4}	84.3 ^{+0.4}	84.6 ^{+0.5}
MMIM [12]	41.8	84.1	84.1
MMIM + SuCI	42.4 ^{+0.6}	84.9 ^{+0.8}	84.8 ^{+0.7}
DMD [21]	41.0	83.3	83.2
DMD + SuCI	42.2 ^{+1.2}	84.6 ^{+1.3}	84.5 ^{+1.3}

The size d_s of each subject confounder is 325, 409, and 456 on MOSI, MOSEI, and UR_FUNNY, respectively. We implement the selected methods and SuCI on NVIDIA Tesla A800 GPUs utilizing the PyTorch toolbox [29], where other training settings are aligned to their original protocols, including the optimizer, additional loss, batch size, learning rate, etc.

4.4 Comparison with State-of-the-art Methods

We compare the SuCI-based models with extensive SOTA methods, including EF-LSTM, LF-LSTM, C-MFN [13], Graph-MFN [60], TFN [59], MFM [43], RAVEN [44], MCTN [34], TCSP [45], PMR [28], and FDMER [48]. The core observations are shown below.

Results on MOSI Benchmark. (i) From Table 1, SuCI consistently improves the performance of the selected methods on all metrics. Concretely, the overall gains of Acc_7 , Acc_2 , and $F1$ scores among the five models increased by 4.8%, 4.8%, and 4.6%, respectively. These improvements confirm that our module can break through the performance bottlenecks of most baselines in a model-agnostic manner. **(ii)** SuCI can bring more favorable gains for decoupled learning-based efforts. For instance, MISA and DMD achieve salient relative improvements among different metrics of 1.8%~3.5% and 1.6%~2.9%, respectively. A reasonable explanation is that the decoupling pattern diffuses the spurious semantics caused by subject confounders in multiple feature subspaces. In this case, SuCI’s de-confounding ability is more effective. **(iii)** We also find that the SuCI-based Self-MM is a slight increment. The potential reason is that the unimodal prediction branches of the vanilla model trigger accidental leakage of backdoor effects [30], thus weakening our causal intervention. **(iv)** Compared to recent PMR

Table 2: Comparison results of different models on the MOSEI benchmark.

Methods	$Acc_7 \uparrow$ (%)	$Acc_2 \uparrow$ (%)	$F1 \uparrow$ (%)
EF-LSTM	47.4	78.2	77.9
LF-LSTM	48.8	80.6	80.6
Graph-MFN [60]	45.0	76.9	77.0
RAVEN [44]	50.0	79.1	79.5
MCTN [34]	49.6	79.8	80.6
TCSP [45]	-	82.8	82.7
PMR [28]	52.5	83.3	82.6
FDMER [48]	53.8	83.9	83.8
MuIT [42]	51.2	82.1	81.9
MuIT + SuCI	52.4 ^{+1.2}	83.2 ^{+1.1}	82.9 ^{+1.0}
MISA [9]	51.3	82.3	82.3
MISA + SuCI	52.6 ^{+1.3}	83.5 ^{+1.2}	83.2 ^{+0.9}
Self-MM [58]	52.9	83.9	83.8
Self-MM + SuCI	53.6 ^{+0.7}	84.2 ^{+0.3}	84.2 ^{+0.4}
MMIM [12]	53.7	84.4	84.3
MMIM + SuCI	54.4 ^{+0.7}	85.5 ^{+1.1}	85.2 ^{+0.9}
DMD [21]	53.5	84.1	84.0
DMD + SuCI	54.6 ^{+1.1}	85.8 ^{+1.7}	85.7 ^{+1.7}

Table 3: Comparison results of different models on the UR_FUNNY benchmark.

Methods	Context	Punchline	$Acc_2 \uparrow$ (%)
C-MFN [13]	✓		58.45
C-MFN [13]		✓	64.47
TFN [59]		✓	64.71
LMF [27]		✓	65.16
C-MFN [13]	✓	✓	65.23
FDMER [48]		✓	70.55
MuIT [42]		✓	66.65
MuIT + SuCI		✓	67.88 ^{+1.23}
MISA [9]		✓	67.34
MISA + SuCI		✓	68.96 ^{+1.62}
Self-MM [58]		✓	68.77
Self-MM + SuCI		✓	69.72 ^{+0.95}
MMIM [12]		✓	69.53
MMIM + SuCI		✓	70.92 ^{+1.39}
DMD [21]		✓	68.70
DMD + SuCI		✓	70.84 ^{+2.14}

and FDMER with complex network stacking and massive parameters [28, 48], MMIM achieves the best results by equipping our efficient SuCI.

Results on MOSEI Benchmark. Table 2 provides performance comparison results on MOSEI. **(i)** The SuCI-based models outperform the vanilla methods by large margins on all evaluation metrics. For example, SuCI helps the latest DMD (CVPR 2023) to achieve new SOTA performance with considerable absolute gains of 1.1%, 1.7%, and 1.7% in Acc_7 , Acc_2 , and $F1$ scores, respectively. These observations demonstrate the broad applicability and usefulness of our module in removing the subject-related prediction bias. **(ii)** The improvements provided by SuCI on MOSEI are more significant than those on MOSI. The plausible deduction is that MOSEI contains richer subjects and their highly idiosyncratic multimodal utterances in various scenarios. Thus, SuCI can more accurately remove spurious correlations caused by appropriately extracted subject confounders and offer sufficient gains.

Table 4: Cross-dataset evaluation results of SuCI-based models trained on the MOSI training set and tested on the MOSEI testing set.

Methods	$Acc_7 \uparrow$ (%)	$Acc_2 \uparrow$ (%)	$F1 \uparrow$ (%)
MuT [42]	46.9	77.6	77.4
MuT + SuCI	48.5 ^{+1.6}	80.2 ^{+2.6}	80.3 ^{+2.9}
MISA [9]	46.6	77.2	77.1
MISA + SuCI	48.3 ^{+1.7}	78.9 ^{+1.7}	79.4 ^{+2.3}
Self-MM [58]	47.7	78.5	78.3
Self-MM + SuCI	48.2 ^{+0.5}	79.5 ^{+1.0}	79.6 ^{+1.3}
MMIM [12]	49.3	79.6	79.3
MMIM + SuCI	51.8 ^{+2.5}	82.5 ^{+2.9}	82.4 ^{+3.1}
DMD [21]	48.9	80.8	80.7
DMD + SuCI	51.6 ^{+2.7}	82.4 ^{+1.6}	82.4 ^{+1.7}

Table 5: Cross-dataset evaluation results of SuCI-based models trained on the MOSEI training set and tested on the MOSI testing set.

Methods	$Acc_7 \uparrow$ (%)	$Acc_2 \uparrow$ (%)	$F1 \uparrow$ (%)
MuT [42]	37.4	80.2	79.9
MuT + SuCI	38.7 ^{+1.3}	81.7 ^{+1.5}	81.5 ^{+1.6}
MISA [9]	37.8	80.5	80.7
MISA + SuCI	39.0 ^{+1.2}	82.2 ^{+1.7}	82.3 ^{+1.6}
Self-MM [58]	38.9	82.0	82.1
Self-MM + SuCI	39.5 ^{+0.6}	82.7 ^{+0.7}	82.4 ^{+0.3}
MMIM [12]	39.3	82.5	82.5
MMIM + SuCI	41.1 ^{+1.8}	83.4 ^{+0.9}	83.3 ^{+0.8}
DMD [21]	38.6	81.6	81.4
DMD + SuCI	40.6 ^{+2.0}	83.0 ^{+1.4}	82.9 ^{+1.5}

Results on UR_FUNNY Benchmark. As shown in Table 3, we mainly show the detection results using the target punchline for fair comparisons with other works. **(i)** Intuitively, the SuCI-based models achieve consistent performance increases and accomplish competitive and better results than previous methods. These substantial improvements imply the necessity of performing subject deconfounded training in detecting human humor. **(ii)** In particular, MMIM and DMD equipped with SuCI yield absolute gains of 1.39% and 2.14%, achieving new SOTAs with the Acc_2 of 70.92% and 70.84%, respectively.

4.5 Cross-dataset Evaluation

Since MOSI and MOSEI benchmarks have the same annotation protocol, we establish cross-dataset evaluations for MOSI-training→MOSEI-testing and MOSEI-training→MOSI-testing in Tables 4 and 5, respectively. The design intuition is that exploring prediction performance on testing data with different distributions than the training data (*i.e.*, out-of-distribution, OOD) helps verify confounding effects and model generalizability. The five vanilla methods show severe performance deterioration compared to the results in the Independent Identically Distributed (IID) setting from Tables 1 and 2. For instance, the testing results on MOSEI and MOSI decreased by the average Acc_7 of 4.64% and 2.42% across all methods. This is inevitable since spurious correlations between trained models and specific subjects are exacerbated and amplified in uninitiated subjects under the OOD setting. Fortunately, our SuCI significantly improves the results of all models in cross-dataset evaluations. These substantial gains confirm that our module favorably mitigates the subject variation problem and enhances the generalizability and robustness of the vanilla models.

4.6 Ablation Studies

In Table 6, we perform systematic ablation studies to evaluate the impact of all components in SuCI. We report results for the Acc_2 metrics due to similar trends for the other metrics. The core observations are as follows.

Table 6: Ablation study results on the three benchmarks. “w/” and “w/o” are short for the with and without, respectively.

Setting	MOSI		MOSEI		UR FUNNY	
	MISA [9]	DMD [21]	MISA [9]	DMD [21]	MISA [9]	DMD [21]
Vanilla Method	81.8	83.3	82.3	84.1	67.34	68.70
+ The Proposed SuCI	83.3	84.6	83.5	85.8	68.96	70.84
Necessity of Subject Feature Learning						
w/o Dynamic Fusion Mechanism	82.9	84.2	83.2	85.3	68.64	70.67
w/o Subject Discriminator	82.2	83.8	82.7	85.0	68.57	69.69
w/o Task Discriminator	82.6	84.1	82.9	85.3	68.62	70.44
Importance of Different Modalities						
w/o Text Modality	82.4	83.6	82.7	84.6	68.25	69.38
w/o Visual Modality	82.9	84.3	83.1	85.4	68.62	69.94
w/o Audio Modality	82.7	84.1	83.0	85.1	68.77	70.35
Rationality of Confounder Dictionary						
w/ Random \mathbf{Z}	79.3	81.0	78.2	79.9	62.46	84.05
w/ Clustered \mathbf{Z}	82.8	83.7	82.9	85.0	67.98	69.63
Effectiveness of Adaptive Aggregation						
w/o ψ_i	82.7	84.2	83.1	85.4	68.45	70.32
w/o $p(\mathbf{z}_i)$	83.0	84.5	83.4	85.6	68.73	70.66

Necessity of Subject Feature Learning. (i) We first replace our dynamic fusion mechanism with the average pooling operation along the frame length to obtain refined representations \mathbf{p}_m . The insufficient gains on all benchmarks suggest that assigning adaptive weights based on the distinct frame element contributions in multimodal sequences facilitates better capturing subject-related semantics. (ii) Subsequently, we separately remove the subject and task discriminators to investigate the role of feature disentanglement. Intuitively, the subject discriminator provides substantial gains for both methods since it supervises the generator to yield discriminative subject features \mathbf{s} that are better used for confounder construction. (iii) The task discriminator is equally critical as it ensures that task-related information is excluded from \mathbf{s} to distill the pure subject bias.

Importance of Different Modalities. (i) When the text, visual, and audio modalities from the subjects are removed separately in de-confounded training, the improvements in SuCI for the baselines show significant deterioration. These decreased results confirm that subject-specific spurious characteristics are transmitted in multimodal utterances and that considering the complete modalities is necessary. (ii) The reason for the pronounced effect of the text modality may be the adverse statistical shortcuts caused by the highly uneven distribution of textual words across the samples of distinct subjects [39], which is a confounder inducer. Also, the impacts of visual and audio modalities are equally essential.

Rationality of Confounder Dictionary. We provide two candidates of the same size as the default confounder dictionary \mathbf{Z} to evaluate the rationality of our confounder construction. These two alternative dictionaries are obtained by random initialization and unsupervised K-Means++ clustering [1]. (i) The random \mathbf{Z} would significantly impair the performance and even underperform the vanilla methods, justifying the proposed subject prototypes as confounders. (ii) The performance gains of the clustered \mathbf{Z} are sub-optimal due to the lack of

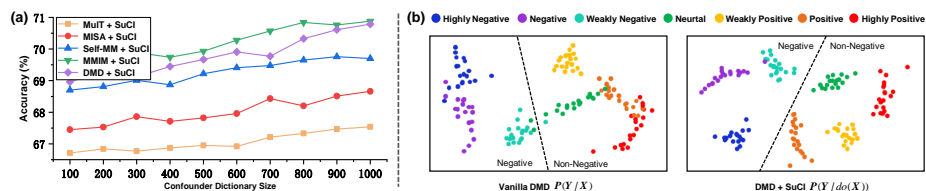


Fig. 4: (a) Ablation study results for the number of subject confounders on the UR_FUNNY benchmark. Similar trends are observed on other benchmarks. (b) Quantitative results (*i.e.*, binary or seven classifications) of vanilla and SuCI-based DMD.

subject-specific information supervision, leading to the indistinguishability and coupling of confounding effects across different subjects.

Effectiveness of Adaptive Aggregation. Here, the adaptive aggregation strategy is explored by eliminating the attention weights ψ_i and the prior probabilities $p(z_i)$ in $\mathbb{E}[h(z)]$, respectively. The consistent performance drops on all benchmarks imply that characterizing the importance and proportion of each subject confounder is indispensable for achieving effective causal intervention based on subject debiasing.

Impact of Subject Confounder Number. Finally, we test the impact of different numbers of subject confounders on SuCI performance in Fig. 4(a). The SuCI-based models all exhibit overall rising gain trends as the training subjects increase (*i.e.*, the number of used human subjects from 100 to 1,000). These findings suggest that sufficient stratified confounders facilitate better backdoor adjustment implementation and accurate average causal effect estimation.

4.7 Qualitative Evaluation

To show the difference between the model approximate $P(\mathbf{Y}|\mathbf{X})$ and $P(\mathbf{Y}|do(\mathbf{X}))$, we randomly select 20 samples in each sentiment category on MOSEI for visualization. As Fig. 4(b) shows, the sample distributions from the different categories of the vanilla baseline prediction usually appear confounded and fragmented. In comparison, the causality-based SuCI improves the predicted results so that the samples in the same category are more compact and different categories are well separated. The observation suggests that our causal intervention promotes discriminative predictions by mitigating the subject prediction bias.

5 Conclusion

This paper is the first to reveal the long-neglected subject variation problem in MIU tasks and identify subjects as essentially harmful confounders from a causal perspective. Thus, we present a subject causal intervention module (SuCI) to remove the prediction bias caused by the subject-specific spurious correlations. Extensive experiments show the broad applicability of SuCI in diverse methods.

References

1. Bahmani, B., Moseley, B., Vattani, A., Kumar, R., Vassilvitskii, S.: Scalable k-means++. arXiv preprint arXiv:1203.6402 (2012) [13](#)
2. Baltrušaitis, T., Robinson, P., Morency, L.P.: Openface: an open source facial behavior analysis toolkit. In: 2016 IEEE Winter Conference on Applications of Computer Vision (WACV). pp. 1–10. IEEE (2016) [9](#)
3. Calefato, F., Lanubile, F., Novielli, N.: Emotxt: A toolkit for emotion recognition from text. In: 2017 Seventh International Conference on Affective Computing and Intelligent Interaction Workshops and Demos (ACIIW). pp. 79–80. IEEE (2017) [1](#)
4. Castro, S., Hazarika, D., Pérez-Rosas, V., Zimmermann, R., Mihalcea, R., Poria, S.: Towards multimodal sarcasm detection (an `_obviously_` perfect paper). arXiv preprint arXiv:1906.01815 (2019) [1](#), [3](#)
5. Chen, Y., Chen, D., Wang, T., Wang, Y., Liang, Y.: Causal intervention for subject-deconfounded facial action unit recognition. In: Proceedings of the AAAI Conference on Artificial Intelligence (AAAI). vol. 36, pp. 374–382 (2022) [2](#)
6. Cruz, A.C., Bhanu, B., Thakoor, N.S.: Vision and attention theory based sampling for continuous facial emotion recognition. IEEE Transactions on Affective Computing **5**(4), 418–431 (2014) [1](#)
7. Dasgupta, I., Wang, J., Chiappa, S., Mitrovic, J., Ortega, P., Raposo, D., Hughes, E., Battaglia, P., Botvinick, M., Kurth-Nelson, Z.: Causal reasoning from meta-reinforcement learning. arXiv preprint arXiv:1901.08162 (2019) [4](#)
8. Degottex, G., Kane, J., Drugman, T., Raitio, T., Scherer, S.: Covarep—a collaborative voice analysis repository for speech technologies. In: IEEE International Conference on Acoustics, Speech and Signal Processing (ICASSP). pp. 960–964. IEEE (2014) [9](#)
9. Devamanyu, H., Roger, Z., Soujanya, P.: Misa: Modality-invariant and-specific representations for multimodal sentiment analysis. In: Proceedings of the 28th ACM International Conference on Multimedia (ACM MM). vol. 34, p. 1122–1131 (2020) [2](#), [4](#), [9](#), [10](#), [11](#), [12](#), [13](#)
10. Du, Y., Yang, D., Zhai, P., Li, M., Zhang, L.: Learning associative representation for facial expression recognition. In: IEEE International Conference on Image Processing (ICIP). pp. 889–893 (2021) [1](#)
11. Glymour, M., Pearl, J., Jewell, N.P.: Causal inference in statistics: A primer. John Wiley & Sons (2016) [3](#), [6](#)
12. Han, W., Chen, H., Poria, S.: Improving multimodal fusion with hierarchical mutual information maximization for multimodal sentiment analysis. arXiv preprint arXiv:2109.00412 (2021) [2](#), [3](#), [9](#), [10](#), [11](#), [12](#)
13. Hasan, M.K., Rahman, W., Zadeh, A., Zhong, J., Tanveer, M.I., Morency, L.P., et al.: Ur-funny: A multimodal language dataset for understanding humor. arXiv preprint arXiv:1904.06618 (2019) [2](#), [3](#), [5](#), [9](#), [10](#), [11](#)
14. Hendrycks, D., Gimpel, K.: Gaussian error linear units (gelus). arXiv preprint arXiv:1606.08415 (2016) [7](#)
15. Huang, W., Liu, H., Bowman, S.R.: Counterfactually-augmented snli training data does not yield better generalization than unaugmented data. arXiv preprint arXiv:2010.04762 (2020) [4](#)
16. iMotions: Facial expression analysis (2017) [9](#)
17. Jones, B.D.: Bounded rationality. Annual review of political science **2**(1), 297–321 (1999) [6](#)

18. Lei, Y., Yang, D., Li, M., Wang, S., Chen, J., Zhang, L.: Text-oriented modality reinforcement network for multimodal sentiment analysis from unaligned multimodal sequences. arXiv preprint arXiv:2307.13205 (2023) [2](#)
19. Li, M., Yang, D., Zhang, L.: Towards robust multimodal sentiment analysis under uncertain signal missing. *IEEE Signal Processing Letters* **30**, 1497–1501 (2023) [4](#)
20. Li, S., Deng, W.: Deep facial expression recognition: A survey. *IEEE transactions on affective computing* (2020) [2](#)
21. Li, Y., Wang, Y., Cui, Z.: Decoupled multimodal distilling for emotion recognition. In: *Proceedings of the IEEE/CVF Conference on Computer Vision and Pattern Recognition (CVPR)*. pp. 6631–6640 (2023) [2](#), [9](#), [10](#), [11](#), [12](#), [13](#)
22. Liang, P.P., Lyu, Y., Fan, X., Wu, Z., Cheng, Y., Wu, J., Chen, L., Wu, P., Lee, M.A., Zhu, Y., et al.: Multibench: Multiscale benchmarks for multimodal representation learning. arXiv preprint arXiv:2107.07502 (2021) [2](#)
23. Liang, T., Lin, G., Feng, L., Zhang, Y., Lv, F.: Attention is not enough: Mitigating the distribution discrepancy in asynchronous multimodal sequence fusion. In: *Proceedings of the IEEE/CVF International Conference on Computer Vision (ICCV)*. pp. 8148–8156 (2021) [2](#), [4](#)
24. Lin, X., Wu, Z., Chen, G., Li, G., Yu, Y.: A causal debiasing framework for unsupervised salient object detection. In: *Proceedings of the AAAI Conference on Artificial Intelligence (AAAI)*. vol. 36, pp. 1610–1619 (2022) [4](#)
25. Liu, Y., Yang, D., Fang, G., Wang, Y., Wei, D., Zhao, M., Cheng, K., Liu, J., Song, L.: Stochastic video normality network for abnormal event detection in surveillance videos. *Knowledge-Based Systems* p. 110986 (2023) [4](#)
26. Liu, Y., Yang, D., Wang, Y., Liu, J., Song, L.: Generalized video anomaly event detection: Systematic taxonomy and comparison of deep models. arXiv preprint arXiv:2302.05087 (2023) [4](#)
27. Liu, Z., Shen, Y., Lakshminarasimhan, V.B., Liang, P.P., Zadeh, A., Morency, L.P.: Efficient low-rank multimodal fusion with modality-specific factors. arXiv preprint arXiv:1806.00064 (2018) [2](#), [10](#), [11](#)
28. Lv, F., Chen, X., Huang, Y., Duan, L., Lin, G.: Progressive modality reinforcement for human multimodal emotion recognition from unaligned multimodal sequences. In: *Proceedings of the IEEE/CVF Conference on Computer Vision and Pattern Recognition (CVPR)*. pp. 2554–2562 (2021) [2](#), [3](#), [10](#), [11](#)
29. Paszke, A., Gross, S., Chintala, S., Chanan, G., Yang, E., DeVito, Z., Lin, Z., Desmaison, A., Antiga, L., Lerer, A.: Automatic differentiation in pytorch (2017) [10](#)
30. Pearl, J.: Causal inference in statistics: An overview. *Statistics Surveys* **3**, 96–146 (2009) [3](#), [4](#), [5](#), [6](#), [7](#), [10](#)
31. Pearl, J.: *Causality*. Cambridge University Press (2009) [4](#)
32. Pearl, J., et al.: *Models, reasoning and inference*. Cambridge, UK: CambridgeUniversityPress **19**, 2 (2000) [4](#)
33. Pennington, J., Socher, R., Manning, C.D.: Glove: Global vectors for word representation. In: *Proceedings of the 2014 conference on empirical methods in natural language processing (EMNLP)*. pp. 1532–1543 (2014) [9](#)
34. Pham, H., Liang, P.P., Manzini, T., Morency, L.P., Póczos, B.: Found in translation: Learning robust joint representations by cyclic translations between modalities. In: *Proceedings of the AAAI Conference on Artificial Intelligence*. vol. 33, pp. 6892–6899 (2019) [2](#), [4](#), [10](#), [11](#)
35. Qian, C., Feng, F., Wen, L., Ma, C., Xie, P.: Counterfactual inference for text classification debiasing. In: *Proceedings of the 59th Annual Meeting of the Association for Computational Linguistics and the 11th International Joint Conference*

- on Natural Language Processing (Volume 1: Long Papers). pp. 5434–5445 (2021) [2](#), [4](#)
36. Rahman, W., Hasan, M.K., Lee, S., Zadeh, A., Mao, C., Morency, L.P., Hoque, E.: Integrating multimodal information in large pretrained transformers. In: Proceedings of the Conference Association for Computational Linguistics Meeting (ACL). vol. 2020, p. 2359. NIH Public Access (2020) [2](#), [4](#)
 37. Song, M., Bu, J., Chen, C., Li, N.: Audio-visual based emotion recognition-a new approach. In: Proceedings of the IEEE/CVF Conference on Computer Vision and Pattern Recognition (CVPR). pp. II–II (2004) [1](#)
 38. Sun, H., Wang, H., Liu, J., Chen, Y.W., Lin, L.: Cubemlp: An mlp-based model for multimodal sentiment analysis and depression estimation. In: Proceedings of the 30th ACM International Conference on Multimedia (ACM MM). pp. 3722–3729 (2022) [2](#), [4](#)
 39. Sun, T., Wang, W., Jing, L., Cui, Y., Song, X., Nie, L.: Counterfactual reasoning for out-of-distribution multimodal sentiment analysis. In: Proceedings of the 30th ACM International Conference on Multimedia (ACM MM). pp. 15–23 (2022) [4](#), [13](#)
 40. Tang, K., Niu, Y., Huang, J., Shi, J., Zhang, H.: Unbiased scene graph generation from biased training. In: Proceedings of the IEEE/CVF Conference on Computer Vision and Pattern Recognition (CVPR). pp. 3716–3725 (2020) [4](#)
 41. Tian, B., Cao, Y., Zhang, Y., Xing, C.: Debiasing nlu models via causal intervention and counterfactual reasoning. In: Proceedings of the AAAI Conference on Artificial Intelligence (AAAI). vol. 36, pp. 11376–11384 (2022) [2](#)
 42. Tsai, Y.H.H., Bai, S., Liang, P.P., Kolter, J.Z., Morency, L.P., Salakhutdinov, R.: Multimodal transformer for unaligned multimodal language sequences. In: Proceedings of the Conference. Association for Computational Linguistics Meeting (ACL). vol. 2019, p. 6558. NIH Public Access (2019) [2](#), [4](#), [9](#), [10](#), [11](#), [12](#)
 43. Tsai, Y.H.H., Liang, P.P., Zadeh, A., Morency, L.P., Salakhutdinov, R.: Learning factorized multimodal representations. arXiv preprint arXiv:1806.06176 (2018) [2](#), [4](#), [10](#)
 44. Wang, Y., Shen, Y., Liu, Z., Liang, P.P., Zadeh, A., Morency, L.P.: Words can shift: Dynamically adjusting word representations using nonverbal behaviors. In: Proceedings of the AAAI Conference on Artificial Intelligence (AAAI). vol. 33, pp. 7216–7223 (2019) [10](#), [11](#)
 45. Wu, Y., Lin, Z., Zhao, Y., Qin, B., Zhu, L.N.: A text-centered shared-private framework via cross-modal prediction for multimodal sentiment analysis. In: Findings of the Association for Computational Linguistics Meeting (ACL-IJCNLP). pp. 4730–4738 (2021) [10](#), [11](#)
 46. Xu, K., Ba, J., Kiros, R., Cho, K., Courville, A., Salakhutdinov, R., Zemel, R., Bengio, Y.: Show, attend and tell: Neural image caption generation with visual attention. In: International Conference on Machine Learning (ICML). pp. 2048–2057. PMLR (2015) [8](#)
 47. Yang, D., Chen, Z., Wang, Y., Wang, S., Li, M., Liu, S., Zhao, X., Huang, S., Dong, Z., Zhai, P., Zhang, L.: Context de-confounded emotion recognition. In: Proceedings of the IEEE/CVF Conference on Computer Vision and Pattern Recognition (CVPR). pp. 19005–19015 (June 2023) [4](#)
 48. Yang, D., Huang, S., Kuang, H., Du, Y., Zhang, L.: Disentangled representation learning for multimodal emotion recognition. In: Proceedings of the 30th ACM International Conference on Multimedia (ACM MM). p. 1642–1651 (2022) [1](#), [2](#), [4](#), [7](#), [9](#), [10](#), [11](#)

49. Yang, D., Huang, S., Liu, Y., Zhang, L.: Contextual and cross-modal interaction for multi-modal speech emotion recognition. *IEEE Signal Processing Letters* pp. 1–5 (2022) [2](#)
50. Yang, D., Huang, S., Wang, S., Liu, Y., Zhai, P., Su, L., Li, M., Zhang, L.: Emotion recognition for multiple context awareness. In: *Proceedings of the European Conference on Computer Vision (ECCV)*. vol. 13697, pp. 144–162 (2022) [4](#)
51. Yang, D., Huang, S., Xu, Z., Li, Z., Wang, S., Li, M., Wang, Y., Liu, Y., Yang, K., Chen, Z., Wang, Y., Liu, J., Zhang, P., Zhai, P., Zhang, L.: Aide: A vision-driven multi-view, multi-modal, multi-tasking dataset for assistive driving perception. In: *Proceedings of the IEEE/CVF International Conference on Computer Vision (ICCV)*. pp. 20459–20470 (October 2023) [4](#)
52. Yang, D., Kuang, H., Huang, S., Zhang, L.: Learning modality-specific and -agnostic representations for asynchronous multimodal language sequences. In: *Proceedings of the 30th ACM International Conference on Multimedia (ACM MM)*. p. 1708–1717 (2022) [2](#), [4](#)
53. Yang, D., Yang, K., Wang, Y., Liu, J., Xu, Z., Yin, R., Zhai, P., Zhang, L.: How2comm: Communication-efficient and collaboration-pragmatic multi-agent perception. In: *Thirty-seventh Conference on Neural Information Processing Systems (NeurIPS)* (2023) [4](#)
54. Yang, K., Yang, D., Zhang, J., Li, M., Liu, Y., Liu, J., Wang, H., Sun, P., Song, L.: Spatio-temporal domain awareness for multi-agent collaborative perception. In: *Proceedings of the IEEE/CVF International Conference on Computer Vision (ICCV)*. pp. 23383–23392 (October 2023) [4](#)
55. Yang, K., Yang, D., Zhang, J., Wang, H., Sun, P., Song, L.: What2comm: Towards communication-efficient collaborative perception via feature decoupling. In: *Proceedings of the 31th ACM International Conference on Multimedia (ACM MM)*. p. 7686–7695 (2023) [4](#)
56. Yang, X., Zhang, H., Cai, J.: Deconfounded image captioning: A causal retrospect. *IEEE Transactions on Pattern Analysis and Machine Intelligence* (2021) [4](#)
57. Yang, X., Zhang, H., Qi, G., Cai, J.: Causal attention for vision-language tasks. In: *Proceedings of the IEEE/CVF Conference on Computer Vision and Pattern Recognition (CVPR)*. pp. 9847–9857 (2021) [4](#)
58. Yu, W., Xu, H., Yuan, Z., Wu, J.: Learning modality-specific representations with self-supervised multi-task learning for multimodal sentiment analysis. In: *Proceedings of the AAAI Conference on Artificial Intelligence (AAAI)*. vol. 35, pp. 10790–10797 (2021) [2](#), [4](#), [9](#), [10](#), [11](#), [12](#)
59. Zadeh, A., Chen, M., Poria, S., Cambria, E., Morency, L.P.: Tensor fusion network for multimodal sentiment analysis. *arXiv preprint arXiv:1707.07250* (2017) [2](#), [4](#), [10](#), [11](#)
60. Zadeh, A., Pu, P.: Multimodal language analysis in the wild: Cmu-mosei dataset and interpretable dynamic fusion graph. In: *Proceedings of the 56th Annual Meeting of the Association for Computational Linguistics (ACL)* (2018) [2](#), [3](#), [5](#), [9](#), [10](#), [11](#)
61. Zadeh, A., Zellers, R., Pincus, E., Morency, L.P.: Mosi: multimodal corpus of sentiment intensity and subjectivity analysis in online opinion videos. *arXiv preprint arXiv:1606.06259* (2016) [2](#), [3](#), [8](#)
62. Zhang, W., Lin, H., Han, X., Sun, L.: De-biasing distantly supervised named entity recognition via causal intervention. *arXiv preprint arXiv:2106.09233* (2021) [4](#)